

Construction of a Fiber Atlas of the Murine Heart

Stelios Angeli¹, Nicholas Befera², Gary Cofer², G Allan Johnson², and Christakis Constantinides¹

¹University of Cyprus, Nicosia, Nicosia, Cyprus, ²Radiology, Duke University Medical Center, Durham, NC, United States

Introduction: The unique myocardial architecture, comprised of oriented laminar sheets and helical spiral tracts of fibers, accounts for its efficient contractile and torsional mechanical function [Jiang 2004, Helm 2005, Peyrat 2007]. The inherent structural-functional associations of the heart also underline the potential significance of fiber tractography in remodeling or cellular disarray, following early, or late pathological states. Diffusion MRI tractography can provide 3-dimensional (3D) mapping of the myofiber structure [Pierpaoli 1996]. This study employs 3D, microscopic, spin-echo, diffusion-weighted MRI [Jiang 2011] to construct a fiber atlas of the ex-vivo, fixed, C57BL/6 murine heart.

Materials and Methods: MRI Imaging: Imaging was performed at the Center of In Vivo Microscopy on a 9.4 T vertical bore magnet equipped with a gradient system able to achieve peak values of 2000 mT/m. Four male C57BL/6 mice (age=8-12 weeks) were perfused with a 10% ProHance (Gadoteridol, Bracco Diagnostics Inc., Princeton, NJ)/formalin solution via a jugular venous catheter. Prior to excision, hearts were perfusion-filled with 1.3% agarose gel to prevent chamber collapse.

A 3D Diffusion-weighted Spin Echo (DW-SE) pulse sequence was used to scan the samples with TE and TR set to 11.8 ms and 100 ms respectively. The acquisition matrix was 256x256x256 spanning a 11 mm³ volume resulting in an isotropic voxel size of 43 μm³. Diffusion was encoded using a pair of half sinusoidal gradient lobes of 1600 mT/m in amplitude, 1.3 ms in width and 6.8 ms in separation. One b₀ and six diffusion weighted image stacks were acquired with a b value of 1852 s/mm². All specimens were scanned in a 12x25 mm² (diameterxlength) solenoid radiofrequency coil.

Estimation of Diffusion Tensors: The acquired diffusion weighted image stacks were imported as NIFTI files into Diffusion Toolkit (MGH, Boston, MA) together with the gradient table [0,0,0], [1,1,0], [1,0,1], [0,1,1], [-1, 1, 0], [1, 0, -1], [0 -1,1] and the b-value to calculate the diffusion tensor for each dataset (Figure 1).

Registration: Each diffusion dataset was registered to the b₀ image to correct for residual eddy currents. The registration employed the Advanced Normalization Tools (ANTS, PA, USA) where Large Diffeomorphic Metric Mapping (LDDMM) with Geodesic Symmetric Normalization (SyN) transformation was applied to register each target dataset to a selected template dataset, using the Procrustes alignment methodology [Bookstein 1993], where a template heart is chosen from the population of imaged datasets, and all other hearts are mapped to the template heart. Mutual Information (MI) was defined as the similarity metric of the registered datasets. The quantitative quality of the registration was assessed by estimating the union overlap measure (Jaccard coefficient) [Klein 2009], by summing the myocardial voxels in the target image that match myocardial voxels in the template image over the total number of myocardial voxels (Figure 1).

Tensor – Reorientation – Averaging: The transformation matrix for each dataset (post-registration) was used to reorient the Diffusion Tensor for each dataset in ANTS in accordance to the preservation of the principle direction (PPD) [Alexander 2001]. The registered/reoriented diffusion tensors were then averaged using Log-Euclidean tensor averaging calculus in ANTS according to:

$$\bar{D}_{\log}(X) = \exp\left(\frac{1}{N} \sum_{i=1}^N \log[D_i(X)]\right) \quad Eq.1 \quad \Sigma(X) = \frac{1}{N-1} \sum_{i=1}^N \{vec[\Delta D_i(X)] \cdot vec[\Delta D_i(X)]^T\} \quad Eq.2$$

where $vec(\Delta D_i)$ is the minimal representation of ΔD_i , and Σ is a representation of the covariance matrix in the log-space, as reported earlier in canine [Peyrat 2007]. The norm $\sqrt{Tr[\Sigma(X)]}$ of such covariance matrix was subsequently calculated to estimate the relative variability of the whole diffusion tensor, in accordance to the methodology published earlier [Peyrat 2007].

Fiber Tractography: The calculated mean Diffusion Tensor was then re-imported in Diffusion Toolkit where fiber tracking was performed using an empirically chosen angle threshold of 40° [Wu 2007] and fractional anisotropy, mean diffusivity and helix angle fiber maps were constructed and visualized (Figure 2).

Results and Discussion: Diffeomorphic registration resulted in a union-overlap measure between 88.5-93.6 % for all three mouse datasets, registered to the population template. Fiber tractography led to a mean statistical map resulting in mean fractional anisotropy of 0.25±0.07 and mean diffusivity of 8.7±1.3×10⁻⁴ mm²/s for all hearts. Helix angle orientations ranged between +40° - -60° while the mean variability of the diffusion tensor was found to be 8.1 %. A typical histogram of primary, secondary, and tertiary eigenvalues from a single heart is shown in Figure 2.

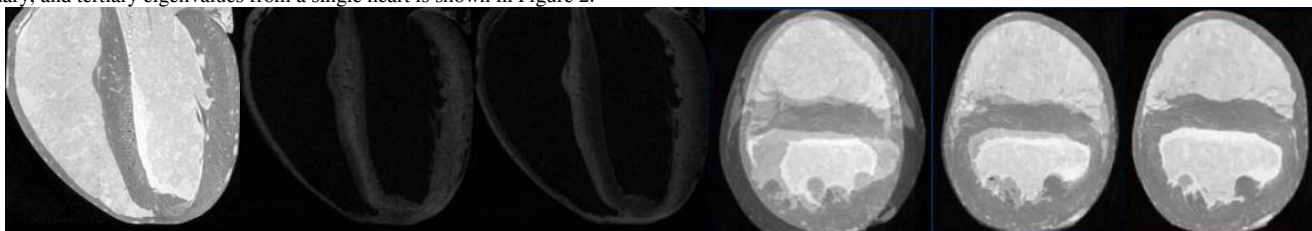


Figure 1: (Left to right) Typical long-axis b₀, b₃, and b₅-weighted diffusion images of the ex-vivo, fixed murine heart; unregistered short-axis, affine- and diffeomorphically-registered short-axis target-template images.

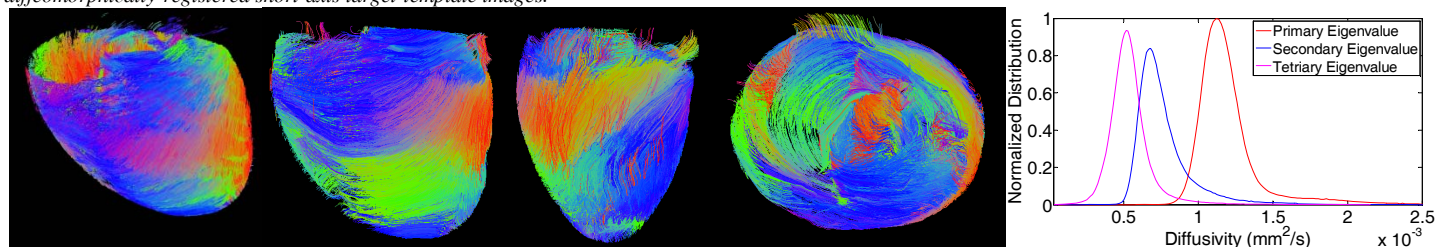


Figure 2: (Left to right) Typical mouse fiber reconstruction (first) and corresponding reconstructions (second, third, fourth) based on the mean diffusion tensor estimate from four mice presented in various orientations with a standard XYZ→RGB directionality color coding scheme; typical histogram distribution of eigenvalues from a single murine heart, showing the relative distributions of unsorted primary, secondary, and tertiary principle values.

Conclusions: Murine myocardial tractography with isotropic resolution of 43-μm of the ex-vivo heart was accomplished in less than 4 hours of data acquisition, sensitized to 6 diffusional directions. Fiber tractography yielded fiber maps that provided in fractional anisotropy amongst the registered hearts and helix angle distributions between +40° - -60°, in agreement with prior published results in humans and canine.

References: 1) Jiang Yi *et al.*, MRM 52:453-460, 2004; 2) Helm PA, *et al.* Circ. Res. 98(1):125-132, 2005; 3) Peyrat JM, *et al.* IEEE TMI 26(11):1500-1514, 2007; 4) Pierpaoli C, *et al.* MRM 36:893-906, 1996; 5) Jiang Y, *et al.* Neuroimage 56:1235-1243, 2011; 6) Bookstein FL, *et al.* Morphometric Tools for Landmark Data, Cambridge Univ. Press, 1993; 7) Klein A, *et al.* Neuroimage 46(3):786-802, 2009. 8) Alexander DC, *et al.* IEEE TMI 20(11):1131-1139, 2001; 9) Wu EX, *et al.* MRI 25:1048-1057, 2007.

Acknowledgements: Support was received (PI: C. Constantinides) from grant IPE/TECNOLOGIA/MHXAN/0609(BE)/05 from the Research Promotion Foundation. All imaging was performed at the Duke Center for In Vivo Microscopy, an NIBIB National Resource (8P41EB015897).